

Cured Shapes of Bi-stable CFRP Composite Laminates with the Side Length Exceeding a Critical Value

Fuhong Dai · Hao Li · Shanyi Du

Received: 29 May 2012 / Accepted: 16 July 2012 / Published online: 31 July 2012
© Springer Science+Business Media B.V. 2012

Abstract Curvature saturation has been observed in bi-stable composite laminates when the side length exceeds a critical value. This is the curvature which the stable cylindrical shell converges to after cooling down. Conventional models of the displacement field fail to predict the correct shapes. This is especially true when the laminate forms a wound-up cylinder which can occur when the longer side is several times the critical length. This paper presents a saturated curvature model to predict the cured shape for bi-stable laminates. The finite element analysis is also carried out to capture the cured shape. Both the analytical model and finite element method give the accurate cured shape. The cured shapes are measured experimentally. The results from the proposed model and finite element analysis are compared with the experimental and show a good agreement.

Keywords Bi-stable · Unsymmetric laminates · Saturated curvature · Cured shape · Rayleigh-Ritz

1 Introduction

Bi-stable composite laminates have been proposed as a method to generate morphing or deployable structures within a range of engineering sectors [1–3]. Bi-stable composite laminates are relatively thin unsymmetric laminates, which exhibit as two structurally stable shapes as a result of thermal mismatch between the composite plies giving rise to a residual stress field during manufacture [4, 5].

Since 1981 several models have been developed to investigate relating variations in composition and architecture to laminate behavior [6–9]. Many factors influencing the cured shape and bi-stable behaviors of unsymmetric laminates, including slippage [10], imperfection [11], fiber orientation [12] and moisture [13], have been investigated.

Recently, high-order and refined analytical models have been proposed to capture the cured cross section shape. Pirrera et al. combined a Ritz model with path-following

F. Dai (✉) · H. Li · S. Du

Center for Composite Materials and Structures, Harbin Institute of Technology, Harbin 150001, China
e-mail: daifh@hit.edu.cn

algorithms to study bi-stable plates' behavior and a refined higher-order model proposed to improve the inherently poor conditioning properties of Ritz approximations of slender structures. The increased degrees of freedom within the model were shown to accurately reflect buckling loads. The complex, experimentally observed snap-through geometry is captured analytically [14, 15]. The convergence properties of orthogonal polynomials were exploited to find detailed solutions for the cross section deformations of unsymmetric laminates [16].

Finite Element Analysis (FEA) has widely been used for calculation of the room temperature shapes and snap-through of unsymmetric laminates [17]. The detail shape change of unsymmetric laminates with complex geometry and the local shape change are able to be captured in finite element simulation. A finite element model including the observed laminate composition was implemented within commercial software ANSYS to predict the cured shapes of the test-laminates by Giddings [18]. The finite element model was also able to predict edge and corner effects which were shown to be related to localized increases in the through-thickness components of shear stress. Predictions from a nonlinear finite element based methodology using the ABAQUS code were used to examine the change in geometry for a subset of configurations, namely, rectangular, trapezoidal and triangular [19]. A characterization using experimental techniques to map the surface profiles of a series of arbitrary layup laminates has been researched and used to validate the existing modelling techniques to predict room-temperature shapes [20].

The works mentioned above are mainly focus on the cured shape and snap-through of unsymmetric laminates with a not-too-long length of side. One of stable shape of the laminate with a very longer length side deforms to be a wound-up cylinder. In the open literatures, the longer bi-stable tapes or tubes are focused on the bi-stability and deployment. Schultz fabricated a series of composite tape springs and explored an analytical model to determine the necessary conditions for neutral stability [21]. Guest and Galletly developed a simple two-parameter model for bi-stable tube and an analytical criterion for stability was derived where bending and twisting are decoupled [22, 23].

The cured shapes of bi-stable laminates are related to the cross section shapes in the directions both orthogonal and parallel to the cylinder directrix. The cross section shape in the direction parallel to the cylindrical directrix has been captured by using high order analytical model or finite element method [14–16, 23]. However, the accurate cured shape of bi-stable laminates with very longer sides, especially in the direction orthogonal to the cylindrical directrix, is still not well understood. With attention switching to the design of mechanisms incorporating bi-stable laminates for actuation, there is an increasing importance placed on the accuracy and the sensitivity of modelling techniques to accurately predict out-of-plane deflections.

In fact, curvature saturation has been observed in bi-stable composite laminates when the side length exceeds a critical value by many researchers. Schlecht used both the finite element and the extended Classical Lamination Theory (CLT) to predict the cured shape based on the temperature dependent material data. He observed the large error of cured shape at the side length of 260 mm. The extended CLT predicts greater displacements in z -direction and smaller displacements in x -direction than the measured values [24]. Dai's investigation also exhibited the similar phenomenon that the extended CLT solution gave a large deviation in cured shape at the side length of 300 mm [25].

This paper focuses on the cured shape prediction of bi-stable laminates with the side length exceeding a critical value. A saturated curvature analytical model and FEA are developed to predict the cured shape for the large length laminates. The experiments are conducted to validate the present modelling techniques.

2 Analytical Model

2.1 Rayleigh-Ritz Model

The Rayleigh-Ritz method is widely used to predict bi-stable unsymmetric laminates’ cured shape. For unsymmetric laminates, the thermally induced directional deformation of the single layer results in large out-of-plane deformations. To take into account the large bi-stable deformations, which are often many times over the laminate thickness, the linear strain–displacement relations must be extended by non-linear terms. It is assumed that the laminate obeys the Kirchhoff hypothesis, and that hypothesis is used in conjunction with the Von Karman approximation to the geometrically nonlinear strain-displacement relations [5–8, 26]:

$$\begin{aligned}
 \varepsilon_x &= \varepsilon_x^0 - z \frac{\partial^2 w}{\partial x^2} = \frac{\partial u^0}{\partial x} + \frac{1}{2} \left(\frac{\partial w}{\partial x} \right)^2 - z \frac{\partial^2 w}{\partial x^2} \\
 \varepsilon_y &= \varepsilon_y^0 - z \frac{\partial^2 w}{\partial y^2} = \frac{\partial v^0}{\partial y} + \frac{1}{2} \left(\frac{\partial w}{\partial y} \right)^2 - z \frac{\partial^2 w}{\partial y^2} \\
 \varepsilon_{xy} &= \varepsilon_{xy}^0 - z \frac{\partial^2 w}{\partial x \partial y} = \frac{1}{2} \left(\frac{\partial u^0}{\partial y} + \frac{\partial v^0}{\partial x} + \frac{\partial w}{\partial x} \frac{\partial w}{\partial y} \right) - z \frac{\partial^2 w}{\partial x \partial y}
 \end{aligned}
 \tag{1}$$

Where the index 0 refers to laminate reference plane, where u^0 and v^0 are the x- and y-reference-surface displacements, w is the z-displacement, and the ε^0 s are the strains at the reference surface, ε_x , ε_y and ε_{xy} the total strains. Total potential energy of the laminate is given by [26]

$$\Pi = \int_{-L_x/2}^{L_x/2} \int_{-L_y/2}^{L_y/2} \int_{-H/2}^{H/2} \left(\frac{1}{2} Q_{11} \varepsilon_x^2 + Q_{12} \varepsilon_x \varepsilon_y + Q_{16} \varepsilon_{xy} \varepsilon_x + \frac{1}{2} Q_{22} \varepsilon_y^2 + Q_{26} \varepsilon_{xy} \varepsilon_y \right. \\
 \left. + \frac{1}{2} Q_{66} \varepsilon_{xy}^2 - (Q_{11} \alpha_x + Q_{12} \alpha_y + Q_{16} \alpha_{xy}) \varepsilon_x \Delta T - \right. \\
 \left. (Q_{12} \alpha_x + Q_{22} \alpha_y + Q_{26} \alpha_{xy}) \varepsilon_y \Delta T - \right. \\
 \left. (Q_{16} \alpha_x + Q_{22} \alpha_y + Q_{66} \alpha_{xy}) \varepsilon_x \Delta T \right) dx dy dz
 \tag{2}$$

Where, L_x and L_y are the two lengths of the laminate and H is the laminate thickness. In Eq. (2), the Q terms represent the transformed reduced stiffness, α is the thermal expansion coefficient.

A practical way to solve this problem is the use of approximate expressions for both curvatures and strains-displacement relations, as functions of unknown coefficients. Geometrical assumptions for the out-of-plane displacements of cross-ply laminates lead to the general second-order approach

$$w(x, y) = \frac{1}{2} (a_0 x^2 + b_0 y^2)
 \tag{3}$$

Where, the coefficients a_0 and b_0 represent the negative curvatures in the x- and y-directions respectively. All three curvatures are assumed constant throughout the plate.

For the description of the in-plane deformations, several approximations can be found in the literatures [5–8, 14–16, 26]. The robustness and reliability of the modelling framework depend on the scaling and conditioning number of the system of solving equations. A high order complete polynomial approximating the displacement field has been proposed by Pirrera and Cerami [14, 16]. They carried out calculations at orders 3, 5, 7, 9 and shown that increasing orders do not lead to major differences in the bifurcation diagram. Actually, by respecting the essential boundary conditions and imposing symmetries, this number can be reduced. Here, the mid-plane displacements are approximated by using the following polynomials with 14 unknown coefficients:

$$\begin{aligned}
 u^0 &= a_1 x + a_2 y + a_3 xy + a_4 x^2 y + a_5 xy^2 + a_6 x^3 + a_7 y^3 \\
 v^0 &= b_1 x + b_2 y + b_3 yx + b_4 y^2 x + b_5 yx^2 + b_6 y^3 + b_7 x^3
 \end{aligned}
 \tag{4}$$

Using the displacement approximations (3) and (4) and in the strain displacement relation (1) substituting the resulting expressions into (2), the total potential energy of the laminate becomes a function dependent on the coefficients a_m, b_m ($m=0,1,\dots,7$).

The principle of the minimum total potential energy requires the first variation to be zero

$$\delta II = \frac{\delta II}{\delta a_m} \delta a_m + \frac{\delta II}{\delta b_m} \delta b_m = 0 \tag{5}$$

To satisfy this condition, every summand in Eq. (5) must be zero, which results in a coupled non-linear algebraic equation system. The equation group is solved with specially-written mathematical software. These solutions should be checked for their stability by means of $\delta^2 II$, which has to be positive for a stable deformation state.

2.2 Saturated Curvature Model

The typical curve of cured curvature with respect to side length could be found everywhere [5–8], as seen in Fig. 1. The point B is the bifurcation point at which the unsymmetric laminate deforms into a cylindrical shell instead of a saddle shape. The cured curvature can be well predicted by using Rayleigh-Ritz model when the side length is short. However, the cured shapes are not represented well by Rayleigh-Ritz model when the side length become longer. The point C is a critical point at which the cured curvature’s saturation occurs. That means the cured curvature always remains constant when the side length of laminates exceeds the critical value. The curvature is defined as the saturated curvature, which can be obtained according to the value at point C in Fig. 1 by conventional Rayleigh-Ritz model.

The Fig. 2 shows the displacements of unsymmetric laminates deforming into a cylinder.

Where, θ is the angular position of point x , as measured from the vertical z -axis, Δx (u^0) is the displacement in x -direction, w is the deflection in z -direction. When the x is small enough, the displacements can be well described by Eqs. (3) and (4). While the x exceeds a critical value and the curvature saturation occurs, the displacements of w and u^0 become periodical functions of x . At this case, the displacements are many times greater than thermal elongation of laminates. Thus, it should be reasonable to assume the in-plane elongation

Fig. 1 Typical bifurcation paths of cured curvature vs. side length of unsymmetric laminates

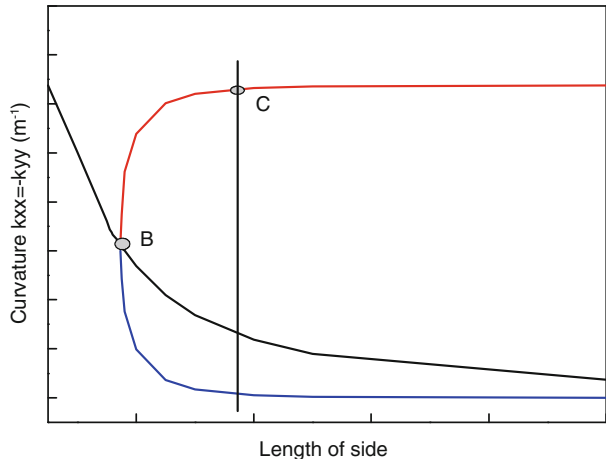
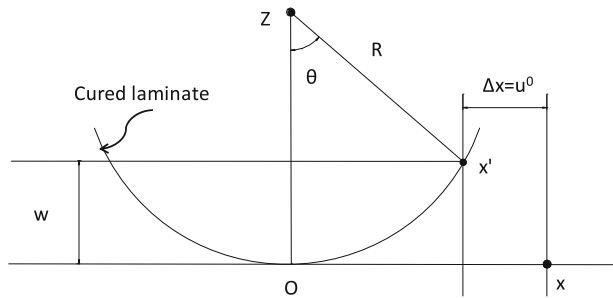


Fig. 2 The displacements of unsymmetric laminates deforming into a cylinder



strain negligible. To explain the periodical displacement fields, a modified displacement fields, termed as the saturated curvature models, are given by

$$\begin{aligned}
 u_{sc}^0 &= \frac{1}{R} \text{Sin}(a_s x) - x \\
 w_{sc}^0 &= R - R \text{Cos}(a_s x)
 \end{aligned}
 \tag{6}$$

Where u_{sc}^0 is the displacement in x-direction, and w_{sc}^0 is the deflection in z-direction, R is equal to $1/a_s$, a_s is the saturated curvature which is determined by the change of cured curvature that remains in range of 0.01 as the side length is increased by 10 %. The expressions of u_{sc}^0 and w_{sc}^0 are used to describe the deformed shape when the side length exceeds the critical value.

3 Finite Element Analysis

The commercial finite element code ABAQUS is here employed to predict the cured shape. ABAQUS offers two procedures, in which both RIKS and STABILIZE methodologies are capable of solving a nonlinear system of equations. The cool-down analysis predicts the various equilibrium configurations. The physical process itself takes a considerable time to complete (a few hours depending on the curing cycle that the material requires) and therefore it can be considered as a quasi-static process. A ‘*Static’ step was used to perform a non-linear static analysis and a ‘*Static, stabilize’ step was used to perform the pseudo-dynamic non-linear analysis. The cool-down was simulated by applying an initial temperature and a final temperature to all of the nodes of the model.

4 Experiments

Several experimental studies have been carried out on bi-stable laminates made of CFRP. The material system is T300/5222A prepreg and its properties are given in Table 1.

The prepregs are put on a aluminum tool and into a vacuum bag first, then they are cured in the autoclave at cured temperature 180 °C and cooled to room temperature 20 °C. Figure 3

Table 1 Thermo-mechanical properties of CFRP

CFRP	E11=137.47 GPa, E22=10.07 GPa, G12=7.17 GPa, ν_{12} =0.23, α_{11} =0.37×10-6/°C, α_{22} =24.91×10-6/°C, Thickness=0.125 mm
------	--



Fig. 3 Manufactured laminates

presents seven manufactured laminates. All the laminates have the same layups $[0/90]$ with dimensions of 140×140 mm, 300×50 mm, 300×70 mm, 300×100 mm, 300×300 mm, 500×100 mm, 1000×200 mm, seen Fig. 3. The laminates with 300 mm length and different widths of 300 mm, 100 mm, 70 mm, 50 mm are used to examine the width effect on the cured shape.

The section shape in the direction orthogonal to the cylindrical directrix were accurately measured. The three laminates with the length of 300 mm and different widths of 50 mm, 70 mm and 100 mm, as shown in Fig. 4, have the nearly same arc lengths after defroming into cylindrical shapes, but a little differences in curvature, $13.09, 13.17$ and 12.87 m^{-1} , respectively.

5 Results

In order to understand the differences between the Eqs. (3, 4) and Eq. (6), the displacements from Rayleigh-Ritz model and saturated curvature model are compared in Figs. 5 and 6. The horizontal coordinate x represents the distance from the original point to the position at the x as

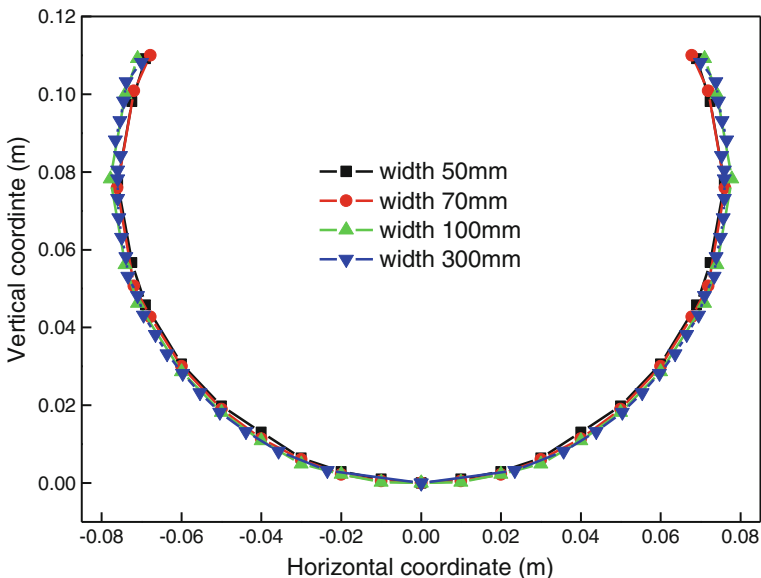


Fig. 4 Measured cross section shape of laminates with the length of 300 mm and different widths

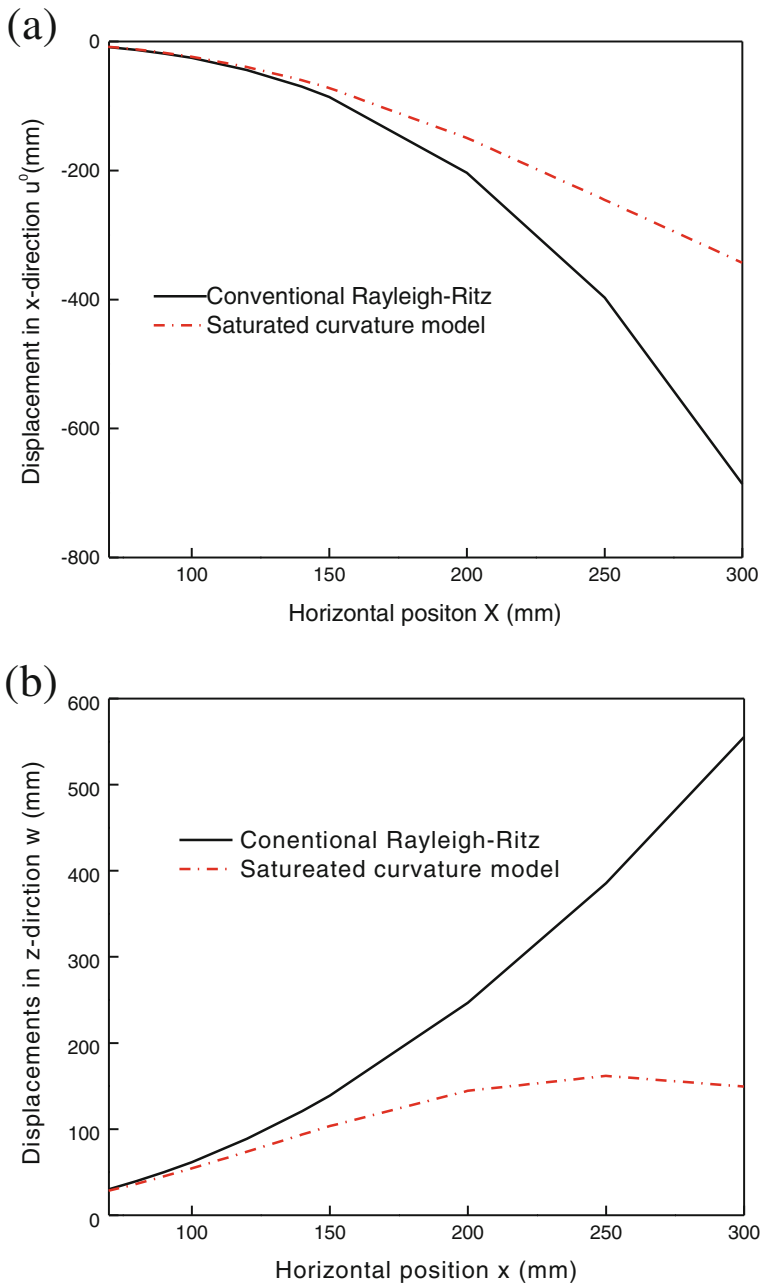
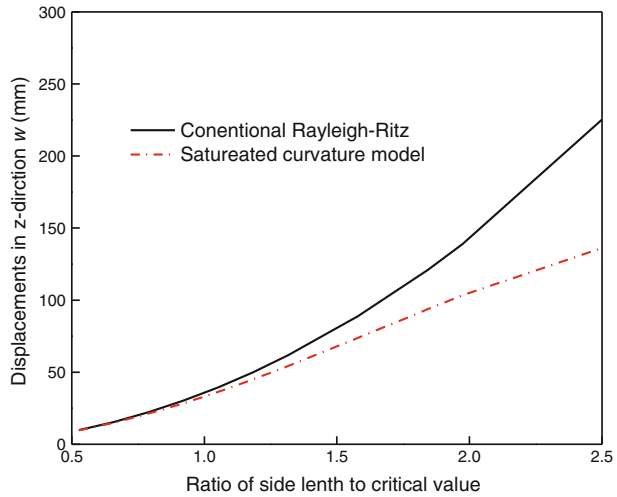


Fig. 5 Comparisons of displacements from conventional Rayleigh-Ritz and saturated curvature model

shown in Fig. 2. Both Rayleigh-Ritz model and saturated curvature model give the almost same prediction of displacement filed at the very small x value. The differences between the two models increase as the horizontal coordinate increases. As mentioned above, the conventional Rayleigh-Ritz model is a single function on the horizontal position x , while the actual

Fig. 6 The difference of displacements between conventional Rayleigh-Ritz and saturated curvature models

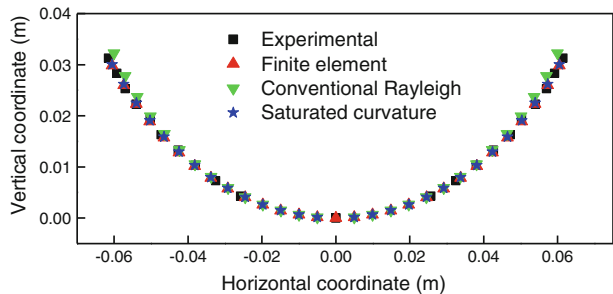


displacements are periodical functions on the horizontal position x . Actually, the cured cylindrical shell has a saturated curvature of 13.17 m^{-1} and a radius of cured cylinder of 76 mm, which is obtained according to the curvature at point C in Fig. 1. The differences between two models increase rapidly at the length exceeding a critical value of 152 mm where Side-length To Critical-Value Ratio (STCR) is greater than 1.0.

The cross section shape of the laminate with the dimension of $140 \times 140 \text{ mm}$ and a STCR of 0.92, is plotted in Fig. 7. The cured shape from the experiment, finite element simulation, predictions of conventional Rayleigh-Ritz and saturated curvature models agree well. The finite element and the curvature saturated model give nearly consistent results which is a little less than the experimental value. The conventional Rayleigh-Ritz model gives a little larger deflection and smaller horizontal displacement.

The cured shapes of laminates with dimensions of $300 \times 300 \text{ mm}$, $500 \times 100 \text{ mm}$ and $1000 \times 200 \text{ mm}$ are respectively shown in Figs. 8, 9 and 10. The STCRs with regard to the side length of 300 mm, 500 mm and 1000 mm are respectively 1.97, 3.29 and 6.58. Again, the good agreements between the experiment and the three predictions by using FEM, Rayleigh-Ritz and saturated curvature model are found at the small length with a STCR less than 1.0. The difference between the experiment and Rayleigh-Ritz model increases

Fig. 7 Cross section shape of the laminate with the dimension of $140 \times 140 \text{ mm}$



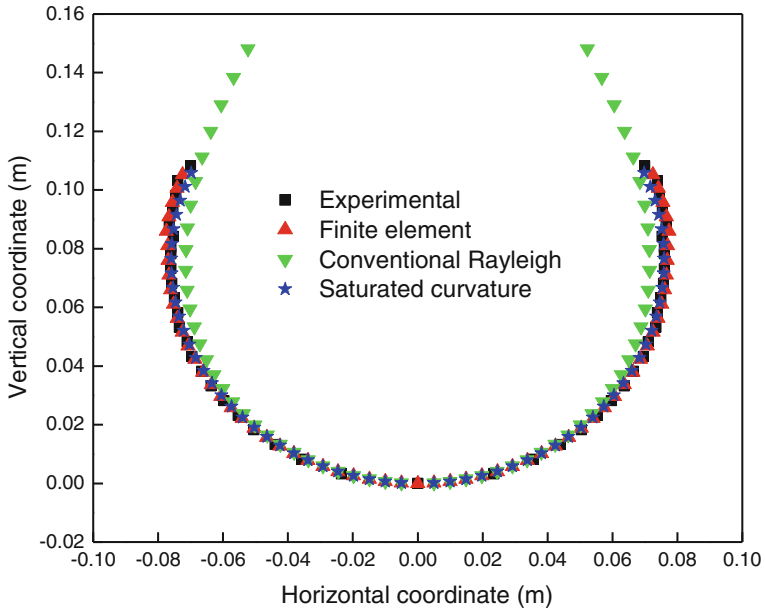


Fig. 8 Cross section shape of the laminate with the dimension of 300×300 mm

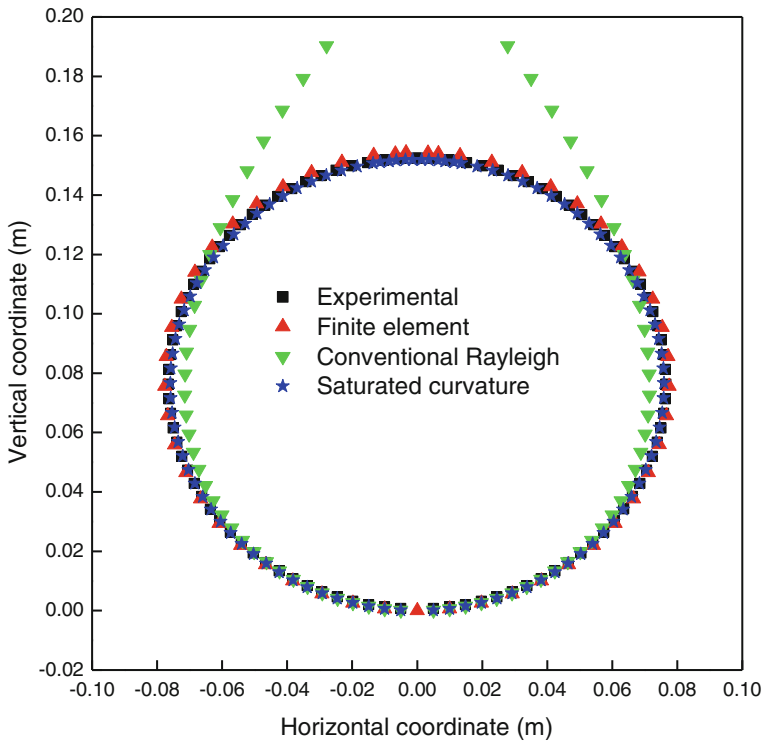


Fig. 9 Cross section shape of the laminate with the dimension of 500×100 mm

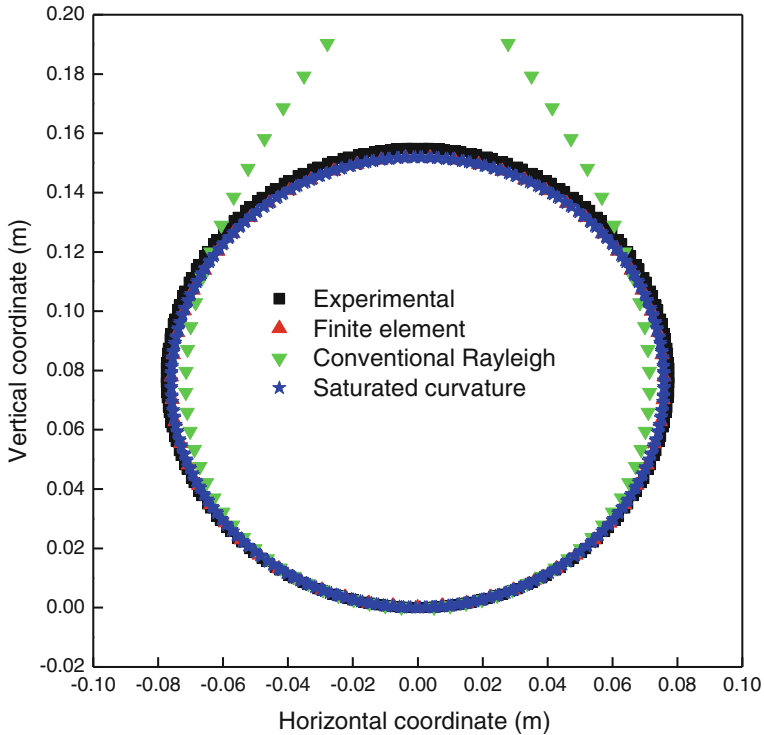


Fig. 10 Cross section shape of the laminate with the dimension of 1000×200 mm

greatly when the side length is greater than the critical value. The similar results were also reported by Schlecht [24] and Dai [25]. When STCR exceeds 2.0, the solutions from conventional Rayleigh-Ritz model completely diverge to the correct cured shape. It can be found that the unsymmetric laminates deform into a wound-up cylinder when the side length is many times greater than the critical value. The coiled cross section shape is captured by FEM and saturated curvature model instead of conventional Rayleigh-Ritz model.

To examine the accuracy by the three methods, FEM, conventional Rayleigh-Ritz and saturated curvature model, the coordinates of points at the end of side are listed in Table 2. There are four 140×140 mm samples, two 300×300 mm samples, two 500×100 mm samples and two 1000×200 mm samples in experiments. The variations of their measured

Table 2 The coordinates of points at the end of cross section shape

	140×140 mm		300×300 mm		500×100 mm		1000×200 mm	
	X(mm)	Z(mm)	x(mm)	z(mm)	x(mm)	z(mm)	x(mm)	z(mm)
Experiments	31.3±0.4 mm	61.5±0.5 mm	108.2±0.5 mm	70.0±0.5 mm	151.8±0.7 mm	-9.6±0.6 mm	1.1±0.6 mm	13.2±0.8 mm
FEM	29.9 (-1.4)	60.2 (-1.3)	105.3 (-2.9)	72.4 (2.4)	155.0 (3.2)	-6.7 (2.9)	3.5 (2.4)	22.5 (9.3)
Conventional Rayleigh-Ritz	32.3 (-3.0)	60.0 (-1.5)	148.1 (39.9)	97.7 (27.7)	—	—	—	—
Saturated curvature model	30.0 (-1.3)	60.5 (-1.0)	105.8 (-2.4)	69.8 (0.2)	151.4 (-0.4)	-11.4 (-1.7)	13.3 (11.9)	42.9 (29.7)

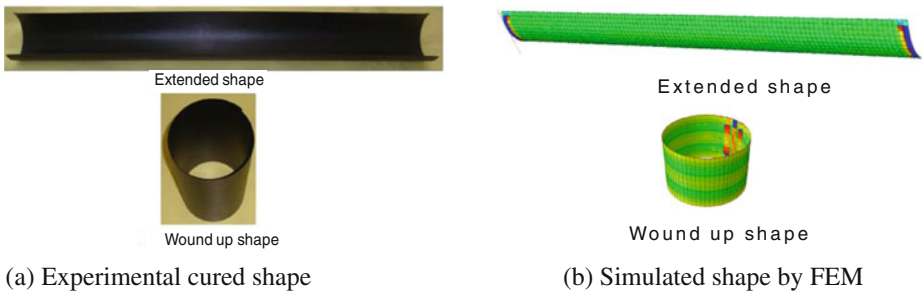


Fig. 11 Two cured shapes of the laminate with the dimension of 1000×200 mm. **(a)** Experimental cured shape. **(b)** Simulated shape by FEM

sizes after cured are included in the table. The value in the brackets represents the difference between the calculated and the experimental results. For the laminate with the dimension of 140×140 mm, the maximum differences of both vertical and horizontal displacements between the experiment and the three methods are less than 1.5 mm. The differences tend to increase with the increasing of side length. The differences of vertical displacements between FEM and the experiment are 2.4, 2.9 and 9.3 mm respectively at the side length of 300, 500 and 1000 mm. The differences of vertical displacements between the saturated curvature model and the experiments are 0.2, -1.7 and 29.7 mm at side length of 300, 500 and 1000 mm. While the differences between conventional Rayleigh-Ritz model and the experiments are too large to represent the correct shape when STCR is greater than 1.97.

The two cured stable shapes of the laminate with the dimension of 1000×200 mm are presented in Fig. 11. One is an extended geometric configuration and another is a wound-up geometric shape. The finite element correctly predict the two stable cured shape.

6 Conclusions

The cured shape of bi-stable laminates with the side length exceeding a critical value has been investigated. The emphasis is put on the cross section shape prediction of the wound-up geometric configuration when the side length is several times the critical length. Conventional analytical models fail to predict the correct shapes of such wound-up configuration. A simple saturated curvature model is used to predict the cured shape for the large length laminates. The finite element analysis is also carried out to capture the cured shape. The comparisons among the experiment, FEM, conventional Rayleigh-Ritz and saturated curvature model show that both the analytical model and finite element method give the accurate cured shape, while conventional Rayleigh-Ritz model fail to give the correct shape when the side length of laminates is very longer. The critical value in saturated curvature model is identified to be the radius of cured cylinder when the curvature saturation occurs. When the side length exceeds the critical value, the saturated curvature model gives correct cross section shape.

Acknowledgements This work was supported by National Natural Science Foundation of China (Grant No.10502016 and 10872058) and the Major State Basic Research Development Program of China (973 Program) under grant No. 2010CB631100.

References

1. Lei, Y.M., Yao, X.F.: Experimental study of bi-stable behaviors of deployable composite structure. *J. Reinf. Plast. Compos.* **29**, 865–873 (2010)
2. Potter, K., Weaver, P., Seman, A.A., et al.: Phenomena in the bifurcation of unsymmetric composite plates. *Composites: Part A* **38**, 100–106 (2007)
3. Peeters, L.J.B., Powell, P.C., Warnet, L.: Thermally-induced shapes of unsymmetric laminates. *J. Compos. Mater.* **30**, 603–626 (1996)
4. Hyer, M.W.: Some observations on the cured shape of thin unsymmetric laminates. *J. Compos. Mater.* **15**, 175–194 (1981)
5. Hyer, M.W.: The room-temperature shapes of four-layer unsymmetric cross-ply laminates. *J. Compos. Mater.* **16**, 318–340 (1982)
6. Ren, L.B., Azar, P.M., Li, Z.N.: Cured shape of cross-ply composite thin shells. *J. Compos. Mater.* **37**(20), 1801–1820 (2003)
7. Jun, W.J., Hong, C.S.: Cured shape of unsymmetric laminates with arbitrary lay-up angles. *J. Reinf. Plast. Compos.* **11**, 1352–1366 (1992)
8. Giddings, P.F.: Modelling of piezoelectrically actuated bi-stable composites. *Mater. Lett.* **65**(9), 1261–1263 (2011)
9. Unger, W.J., Hansen, J.S.: The effect of cooling rate and annealing on residual Stress development in graphite fibre reinforced PEEK laminates. *J. Compos. Mater.* **27**, 108–137 (1993)
10. Cho, M., Kim, M.-H., Choi, H.S., et al.: A study on the room-temperature curvature shapes of unsymmetric laminates including slippage effects. *J. Compos. Mater.* **32**(5), 460–482 (1998)
11. Harper, B.D.: The effects of moisture induced swelling upon the shapes of anti-symmetric cross-ply laminates. *J. Compos. Mater.* **21**, 36–48 (1987)
12. Gigliotti, M., Wisnom, M.R., Potter, K.D.: Loss of bifurcation and multiple shapes of thin [0/90] unsymmetric composite plates subject to thermal stress. *Compos. Sci. Technol.* **64**, 109–128 (2004)
13. Mattioni, F., Weaver, P.M., Friswell, M.I.: Multistable composite plates with piecewise variation of lay-up in the planform. *Int. J. Solid Struct.* **46**(1), 151–164 (2009)
14. Pirrera, A., Avitabile, D., Weaver, P.M.: Bi-stable plates for morphing structures: a refined analytical approach with high-order polynomials. *Int. J. Solid Struct.* **47**, 3412–3425 (2010)
15. Pirrera, A., Avitabile, D., Weaver, P.M.: On the thermally induced bistability of composite cylindrical shells for morphing structures. *Int. J. Solid Struct.* **49**, 685–700 (2012)
16. Cerami, M., Weaver, P.M.: Characterization of unsymmetric cross-ply laminate deflections using orthogonal polynomials. In: 49th AIAA/ASME/ASCE/AHS/ASC Structures, Structural Dynamics, and Materials Conference, Schaumburg, IL, AIAA (2008-1928)
17. Tawfik, S., Tan, X.Y., Ozbay, S., et al.: Anticlastic stability modeling for cross-ply composites. *J. Compos. Mater.* **41**(11), 1325–1338 (2007)
18. Giddings, P.F., Bowen, C.R., Solo, A.I.T., et al.: Bi-stable composite laminates: effects of laminate composition on cured shape and response to thermal load. *Compos. Struct.* **92**, 2220–2225 (2010)
19. Tawfik, S., Stefan, D.D., Armanios, E.: Planform effects upon the bi-stable response of cross-ply composite shells. *Composites: Part A* **42**, 825–833 (2011)
20. Betts, D.N., Salo, A.I.T., Bowen, C.R., et al.: Characterisation and modelling of the cured shapes of arbitrary layup bi-stable composite laminates. *Compos. Struct.* **92**(7), 1694–1700 (2010)
21. Schultz, M.R., Hulse, M.J., Keller, P.N.: Neutrally stable behavior in fiber-reinforced composite tape springs. *Composites: Part A* **39**, 1012–1017 (2009)
22. Guest, S.D., Pellegrino, S.: Analytical models for bi-stable cylindrical shells. *Proc. R. Soc. A* **462**, 839–854 (2006)
23. Galletly, D.A., Guest, S.D.: Bi-stable composite slit tubes. II. A shell model. *Int. J. Solid Struct.* **41**, 4503–4516 (2004)
24. Schlecht, M., Schulte, K.: Advanced calculation of the room-temperature shapes of unsymmetric laminates. *J. Compos. Mater.* **33**(16), 1472–1490 (1999)
25. Dai, F.H., Zhang, B.M., He, X.D., et al.: Numerical and experimental studies on cured shape of thin unsymmetric Carbon/Epoxy laminates. *Key Eng. Mater.* **334–335**, 137–140 (2007)
26. Hufenbach, W., Gude, M.: Analysis and optimisation of multistable composites under residual stresses. *Compos. Struct.* **55**, 319–327 (2002)